ORIGINAL RESEARCH

Newly Identified Peptide, Peptide Lv, Promotes Pathological Angiogenesis

Liheng Shi, PhD;* Min Zhao, MD;* Colette A. Abbey, BS; Shu-Huai Tsai, PhD; Wankun Xie, MD, PhD; Dylan Pham, MS; Samantha Chapman; Kayla J. Bayless, PhD; Travis W. Hein, PhD; Robert H. Rosa Jr MD; Michael L. Ko, PhD, MBA; Lih Kuo, PhD; Gladys Y.-P. Ko, PhD

***Background*—**We recently discovered a small endogenous peptide, peptide Lv, with the ability to activate vascular endothelial growth factor receptor 2 and its downstream signaling. As vascular endothelial growth factor through vascular endothelial growth factor receptor 2 contributes to normal development, vasodilation, angiogenesis, and pathogenesis of various diseases, we investigated the role of peptide Lv in vasodilation and developmental and pathological angiogenesis in this study.

***Methods and Results*—**The endothelial cell proliferation, migration, and 3-dimensional sprouting assays were used to test the abilities of peptide Lv in angiogenesis in vitro. The chick chorioallantoic membranes and early postnatal mice were used to examine its impact on developmental angiogenesis. The oxygen-induced retinopathy and laser-induced choroidal neovascularization mouse models were used for in vivo pathological angiogenesis. The isolated porcine retinal and coronary arterioles were used for vasodilation assays. Peptide Lv elicited angiogenesis in vitro and in vivo. Peptide Lv and vascular endothelial growth factor acted synergistically in promoting endothelial cell proliferation. Peptide Lv–elicited vasodilation was not completely dependent on nitric oxide, indicating that peptide Lv had vascular endothelial growth factor receptor 2/nitric oxide–independent targets. An antibody against peptide Lv, anti-Lv, dampened vascular endothelial growth factor–elicited endothelial proliferation and laser-induced vascular leakage and choroidal neovascularization. While the pathological angiogenesis in mouse eyes with oxygen-induced retinopathy was enhanced by exogenous peptide Lv, anti-Lv dampened this process. Furthermore, deletion of peptide Lv in mice significantly decreased pathological neovascularization compared with their wild-type littermates.

***Conclusions*—**These results demonstrate that peptide Lv plays a significant role in pathological angiogenesis but may be less critical during development. Peptide Lv is involved in pathological angiogenesis through vascular endothelial growth factor receptor 2–dependent and –independent pathways. As anti-Lv dampened the pathological angiogenesis in the eye, anti-Lv may have a therapeutic potential to treat pathological angiogenesis. **(*J Am Heart Assoc*. 2019;8:e013673. DOI: 10.1161/JAHA.119.013673.)**

Key Words: angiogenesis • endothelial cell • vasculogenesis

Formation of new blood vessels occurs under various physiological and pathological conditions. Vascular endothelial growth factor (VEGF)-mediated angiogenesis plays an important role in normal development[1] and wound healing.[2,3] Elevated expression of VEGF and its receptor 2 (VEGFR2) subtype manifests the pathological angiogenesis in diseases with neovascularization, such as metastatic cancers,[4] atherosclerosis,[5] cardiac hypertrophy,[6] myocardial infarction,[7] arthritis,[8] diabetic limb ischemia,[9] and ocular diseases[10–15] including diabetic retinopathy (DR)[15,16] and age-related macular degeneration.[17,18] During angiogenesis, endothelial cells proliferate and migrate out as sprouts from preexisting blood vessels, which then invade the surrounding tissues and form new vascular networks.[19] Therapeutic

From the Department of Veterinary Integrative Biosciences, College of Veterinary Medicine and Biomedical Sciences (L.S., D.P., S.C., M.L.K., G.Y.-P.K.) and Texas A&M Institute for Neuroscience (G.Y.-P.K.), Texas A&M University, College Station, TX; Department of Medical Physiology, Ophthalmic Vascular Research Program (M.Z., S.-H.T., W.X., T.W.H., R.H.R., L.K.) and Department of Molecular and Cellular Medicine (C.A.A., K.J.B.), College of Medicine, Texas A&M University Health Science Center, Bryan, TX; Department of Ophthalmology, Baylor Scott & White Eye Institute, Temple, TX (R.H.R.); Department of Biology, Blinn College, Bryan, TX (M.L.K.).

*Dr Shi and Dr Zhao contributed equally to this work.

Correspondence to: Gladys Y.-P. Ko, PhD, Department of Veterinary Integrative Biosciences, College of Veterinary Medicine and Biomedical Sciences, Texas A&M University, 4458 TAMU, College Station, TX 77843-4458. E-mail: gko@cvm.tamu.edu and Lih Kuo, PhD, Department of Medical Physiology, College of Medicine, Texas A&M University Health Science Center, 8447 Riverside Parkway, Bryan, TX 77807. E-mail: lkuo@tamu.edu

Received June 26, 2019; accepted September 9, 2019.

Clinical Perspective

What Is New?

- Peptide Lv is a newly discovered endogenous angiogenic and vasodilating peptide that is upregulated in conditions with pathological angiogenesis, including early proliferative diabetic retinopathy and oxygen-induced retinopathy.
- An antibody against peptide Lv, anti-Lv, dampens pathological angiogenesis in animals with oxygen-induced retinopathy and decreases laser-induced choroidal neovascularization.

What Are the Clinical Implications?

- Future development of peptide Lv and anti-Lv for therapeutic usage is promising: Peptide Lv can be used for treating diseases such as stroke, ischemia, and atherosclerosis because of its abilities in angiogenesis and vasodilation, and anti-Lv can be used to inhibit pathological neovascularization in tumors and various ocular vascular diseases.

myocardial angiogenesis is a promising therapy to alleviate the heart damage after myocardial infarction.[6,7] At the same time, antiangiogenic approaches, such as anti-VEGF therapies, have been widely used to treat various cancers and diseases associated with pathological angiogenesis.[20] However, the effectiveness varies, and nearly 30% of patients do not respond or become resistant to anti-VEGFs.[21–25] In addition, repetitive treatments with anti-VEGFs are needed to block the recurring pathological angiogenesis, which often leads to unintended side effects.[21,26] One possible explanation is the concurrent upregulation of other angiogenic factors that are insensitive to anti-VEGFs.[18,27–31] Unknown factors that contribute to the resistance and nonresponsiveness to anti-VEGF treatments are yet to be identified.[24] Thus, searching for VEGF-independent angiogenic factors becomes a major quest to conquer the resistance to anti-VEGF treatments and the problems of recurring pathological angiogenesis in these diseases.

We recently discovered a small proangiogenic peptide, peptide Lv, named for its ability to enhance the expression and current amplitudes of L-type voltage-gated calcium channels in cultured photoreceptors and cardiomyocytes.[32,33] Peptide Lv is an endogenous secretory peptide with ≈40 amino acids (human gene ID: 196740, a.a. 55–94; mouse gene ID: 320736, a.a. 55–103) encoded in *Vstm4* (V-set and transmembrane domain containing 4 gene), and its amino acid sequence is highly conserved (>90%) among humans, mice, rats, and chickens.[32,33] Peptide Lv mRNA is expressed in various organs including the eye, heart, brain, liver, spleen, and lung,[32,33] and peptide Lv is detected in retinal neurons and vascular endothelial cells.[33] Peptide Lv exhibits angiogenic properties in vitro by promoting endothelial cell proliferation and activating VEGFR2 and its downstream signaling proteins, including the VEGFR2-coupled tyrosine kinase, extracellular signal-regulated kinase, and protein kinase C.[33] Interestingly, both VEGF and peptide Lv augment L-type voltage-gated calcium channel current amplitudes in cultured cardiomyocytes through VEGFR2 activation.[33] Thus, certain biological actions of peptide Lv are similar to those of VEGF.

While activation of VEGF and VEGFR2 signaling contributes to both developmental angiogenesis and pathological neovascularization,[1,20] the role of peptide Lv in these processes remains unknown. Since peptide Lv is expressed in vascular endothelial cells and is able to activate VEGFR2, we hypothesized that peptide Lv is a proangiogenic modulator. As VEGF via VEGFR2 elicits endothelial nitric oxide (NO)-dependent vasodilation,[34,35] it is not clear whether peptide Lv evokes similar vasomotor activity and signaling. In the present study, the effects of peptide Lv on endothelial proliferation, migration, and sprouting were determined in cultured endothelial cells. The involvement of peptide Lv on vascular development was examined in the chick chorioallantoic membrane (CAM)[36] and the neonatal mouse retina[37] in vivo. The role of peptide Lv in pathological angiogenesis was studied in the oxygen-induced retinopathy (OIR) and laser-induced choroidal neovascularization (CNV) mouse models with peptide Lv inhibition using "anti-Lv," an antibody against peptide Lv, as well as peptide Lv null (peptide $Lv^{-/-}$) mice. We found that peptide Lv and VEGF had synergistic effects in promoting endothelial cell proliferation, but peptide Lv had VEGFR2-independent bioactivities. Furthermore, anti-Lv damped VEGF-elicited endothelial proliferation and laser-induced vascular leakage and CNV. The peptide $Lv^{-/-}$ mice had significantly lower pathological angiogenesis compared with their wild-type (WT) littermates. Our data suggest that peptide Lv is involved in pathological angiogenesis through VEGFR2-dependent and -independent pathways.

Methods

The data that support the findings of this study are available from the co-first authors (L. Shi and M. Zhao) and the co–corresponding authors (L. Kuo and G. Ko) upon reasonable request.

Experimental Animals

The peptide Lv null mice ($PLv^{-/-}$; C57BL/6J background) were generated using the CRISPR-Cas9 genomic editing method at the Texas A&M Institute for Genomic Medicine. The single-guide RNA sequences (CTAAAGTAAAATAAGACGAAGG and AACGCTGTTGGCATCTCGGAGG) were designed to specifically target the second exon of the mouse *Vstm4* gene (encoding the

peptide Lv precursor). The mouse genomic DNAs were isolated from the tails. The entire deletion of exon 2 of *Vstm4* was confirmed by polymerase chain reaction and DNA sequencing. The mice were backcrossed with the WT C57BL/6J mice for 4 generations. The $PLv^{-/-}$ (homozygous), $PLv^{+/-}$ (heterozygous), and $PLv^{+/+}$ WT littermates used in this study were produced at Texas A&M University (College Station, TX). Mice were housed under temperature- and humidity-controlled conditions with 12:12 hours light-dark cycles, and food and water were given ad libitum. Animal experiments using these mice were approved by the Institutional Animal Care and Use Committee of Texas A&M University. Male C57BL/6J mice (6–8 weeks old) obtained from Charles River Laboratories (Charleston, SC) were used for the laser-induced CNV study. These experiments were approved by the Institutional Animal Care and Use Committee of Baylor Scott & White Health. Domestic (Yorkshire) male pigs (8–12 weeks old, 10–15 kg) purchased from Real Farms (San Antonio, TX) were used for the vasodilation study. All procedures using pigs were approved by the Institutional Animal Care and Use Committee of Baylor Scott & White Health.

Peptide Lv and Anti-Lv

Peptide Lv was a custom-made synthetic peptide obtained from Peptide 2.0 (Chantilly, VA). The polyclone antibody specifically against peptide Lv, anti-Lv, was obtained from Biomatik (Cambridge, Ontario, Canada). The murine amino acid sequence used to make peptide Lv and anti-Lv was DSLLAVRWFFAPDGSQEALMVKMTKLRIIQYYGNFSRTANQQRLR LLEE.[32,33] Both peptide Lv and anti-Lv tested negative for endotoxin. The specificity of anti-Lv was verified using spleens excised from the $PLv^{-/-}$, $PLv^{+/-}$, and WT mice.

In Vitro Scratch Gap Migration Assays

The human retinal endothelial cells (RECs; Cell Systems, Kirkland, WA) were maintained in EGM™-2MV BulletKit culture medium (Lonza, Allendale, NJ). The cells were seeded onto 6-well culture plates at 80% confluency and allowed to adhere overnight to form a monolayer. A gap was generated in the monolayer by scratching across the center of the well with a sterile pipette tip. The culture media were exchanged to Opti-MEM (minimal essential media; Thermo Fisher Scientific, Waltham, MA) containing 20% fetal bovine serum (Thermo Fisher Scientific) with or without peptide Lv (400 ng/mL) for 4 additional days to allow RECs to grow. The images were captured every 24 hours at various spots of the gaps using an Olympus IX 71 inverted microscope (Olympus America, Waltham, MA), and the gap distance was measured using the ImageJ software (National Institutes of Health, Bethesda, MD). The linear regression used to determine the REC migration rate was $y=Kx+n$, where x is the specific time point (in hour), y is the mean of the migration distances from different experimental trials at that specific time point (in pixels), and K is the K_{slope}. The linear regression was performed using Origin 9.0 (OriginLab, Northampton, MA).

Three-Dimensional Endothelial Cell Sprouting/Invasion Assays

Primary human umbilical vein endothelial cells (HUVECs; Lonza) were cultured at passages 3 to 6 in 75 cm^2 flasks coated with 1 mg/mL sterile gelatin. The growth medium was previously described in detail[38] and consisted of M199 supplemented with fetal bovine serum, bovine hypothalamic extract, heparin, antibiotics, and gentamycin. Collagen matrices at 2.5 mg/mL contained 1 μmol/L sphingosine 1-phosphate (Avanti Polar Lipids, Alabaster, AL) and type I collagen isolated from rat tails (Pel-Freeze Biologicals, Rogers, AK). Collagen was pipetted into 96-well half area plates (Costar, New York, NY) and equilibrated for 45 minutes. In some groups, peptide Lv was added to collagen matrices at a final concentration of 400 ng/mL before polymerization. Confluent HUVECs were resuspended in M199 and seeded at 30 000 cells per well. Humidified cultures were allowed to invade for 20 to 24 hours at 37°C with 5% CO_2 before fixation in phosphate-buffered saline (PBS) containing 3% glutaraldehyde (Sigma-Aldrich, St. Louis, MO). After overnight fixation, gels were stained with 0.1% toluidine blue in 30% methanol. For invasion density measurements, a minimum of 3 fields were quantified. Each assay was replicated 3 times.

Chick Chorioallantoic Membrane Angiogenesis Assays

Fertilized eggs (*Gallus gallus*) were obtained from the Poultry Science Department, Texas A&M University (College Station, TX). Shell-less (ex ovo) cultures of chicken embryos started at embryonic day 2 (E2)-E3 as previously described.[39–43] At E7-E8, either peptide Lv (10 μL, 500 μg/mL), anti-Lv (1 μg in 10 μL), or PBS (10 μL; vehicle control) was carefully dropped on the surface of chorioallantoic membranes and covered with a small sterile plastic coverslip. Each embryo had 2 to 3 coverslips: a PBS coverslip with a peptide Lv coverslip or an anti-Lv coverslip. At E11-12, the blood vessel images were captured, and the vascular area (as vessel percentage) and vessel length were analyzed using the AngioTool software (National Institutes of Health).

Intravitreal Injections and OIR Mouse Model

To study the effect of peptide Lv on retinal vascular development in early postnatal mice (Figure 1D), mice were

anesthetized at postnatal day 7 (P7) by intraperitoneal injections of Avertin (2% 2,2,2-tribromoethanol and 1.25% tert-amyl alcohol mixture; Thermo Fisher Scientific) solution (12.5 mg/mL) at a dose of 20 μL per 1 g of body weight. A 30-gauge needle was used to puncture a hole in the superior nasal sclera at the level of the pars plana. After a small amount of vitreous was removed through the puncture hole, a Hamilton syringe (Hamilton, Reno, NV) with a 31-gauge blunt needlepoint was inserted at a 45-degree angle through the puncture hole to deliver 2 μL of solution containing 0.5 μg/μL peptide Lv into the vitreous body. The PBS (2 μL) was delivered to the vitreous of the contralateral eye as vehicle control. After intravitreal injections, ophthalmic Tobrex ointment was applied to the eyes to prevent infection. At P14, the mice were euthanized, and the retinas were excised for further analyses.

The OIR procedure was described previously.[44] Briefly, mouse litters were placed in a 75% oxygen chamber from P7 to P12. At P12, the mouse pups were transferred to room air and subjected to the intravitreal injections (2 μL) of PBS (vehicle control) in one eye and peptide Lv (1 μg/μL) or anti-Lv (2 μg/μL) in the contralateral eye. Mice were euthanized at P17, and the retinas were excised for further analyses.

Immunofluorescent Staining and Quantification of Retinal Vasculature

Mouse eyes were excised and fixed with Zamboni's fixative (American Matertech Scientific Inc, Lodi, CA) for 2 hours at 4°C. The retinas were isolated, stained overnight at 25°C with fluorescein isothiocyanate (FITC)-conjugated Isolectin B4 (Sigma-Aldrich) in PBS containing 0.1% Triton X-100 and 1 mmol/L Ca^{2+}, and kept in a dark box. Following 2 hours of wash in PBS, the retinas were cut on the peripheral edge and flat-mounted with the photoreceptor side down onto microscope slides (VWR Scientific, Sugar Land, TX) in ProLong Antifade reagents (Thermo Fisher Scientific). Images were captured at ×10 magnification on a Zeiss Axioplan microscope (Carl Zeiss AG, Oberkochen, Germany), and images were stitched together with the Image Composite Editor software (Microsoft, Seattle, WA) to form whole-mount retinal images.

The whole-mount retinal images were used for quantification of retinal vasculature. For the developmental study, the vascular area (percentage of the total retinal area; %) was quantified using ImageJ (National Institutes of Health). For the OIR experiments, retinal vascular obliteration (avascular and total retinal areas) was analyzed using ImageJ. Neovascularization (the areas of neovascularization tufts) was analyzed using the SWIFT_NV macros in conjunction with ImageJ as previously described.[45] The ratios of vascular obliteration/total retinal area and vascular tufts/total retinal area were first calculated then further normalized against the control (either PBS injected or the WT).

Vasodilation of Retinal and Coronary Arterioles

Domestic (Yorkshire) male pigs (8–12 weeks old, 10–15 kg) purchased from Real Farms (San Antonio, TX) were sedated with Telazol (4–8 mg/kg, intramuscularly; Zoetis, Parsippany, NJ), anesthetized with 2% to 5% isoflurane (Halocarbon, Peachtree Corners, GA), and intubated. The heart and eyes were harvested as described previously.[46,47] The techniques for identification, isolation, cannulation, pressurization, and visualization of the coronary and retinal microvasculature were carried out according to previous descriptions.[46,48] Briefly, individual coronary or retinal arterioles (1–1.5 mm in length; ≈40–60 μm in situ diameter) were dissected from the surrounding cardiac or retinal tissue. The inner diameter of arterioles was recorded using videomicroscopic techniques throughout the experiments as described previously.[47,49,50] The vessels were bathed in physiological salt solution (PSS) containing 1% bovine albumin at 36 to 37°C to allow for the development of stable basal tone.[46] The vasomotor response of these vessels to cumulative administration of peptide Lv (1, 2.5, 5, and 10 μg/mL) was then evaluated. Arterioles were exposed to each concentration of peptide Lv for 2 to 3 minutes until a stable diameter was established. To assess the contribution of NO in the vasodilation to peptide Lv, a second concentration-response curve was evaluated after incubation of vessels with the NO synthase inhibitor N(G)-nitro-L-arginine methyl ester (L-NAME, 10 μmol/L; Sigma-Aldrich) for 30 minutes. At the end of each experiment, the maximum diameter of the vessels was obtained in the presence of calcium-free PSS with 1 mmol/L EDTA (Sigma-Aldrich) and sodium nitroprusside (0.1 mmol/L, Sigma-Aldrich). Diameter changes in response to peptide Lv were normalized to this maximum vasodilation and expressed as % maximum dilation. The n value represents the number of pigs studied (1 vessel per pig; total of 13 pigs studied).

Tetrazolium Dye 3-(4,5-Dimethylthiazol-2-yl)-2, 5-Diphenyltetrazolium Bromide Colorimetric Assays for Cell Proliferation

Human RECs or HUVECs (Cell Application, San Diego, CA) were seeded onto 24-well plates in EGM-2MV BulletKit culture medium (Lonza) and allowed to adhere overnight. The culture media were exchanged to Opti-MEM (Thermo Fisher Scientific) supplemented with 20% fetal bovine serum. VEGF (Abcam, Cambridge, MA) at various concentrations with or without peptide Lv (100 ng/mL) was added to the media, and the cells were continuously incubated for another 48 hours. Cells incubated in the Opti-MEM with 20% fetal bovine serum

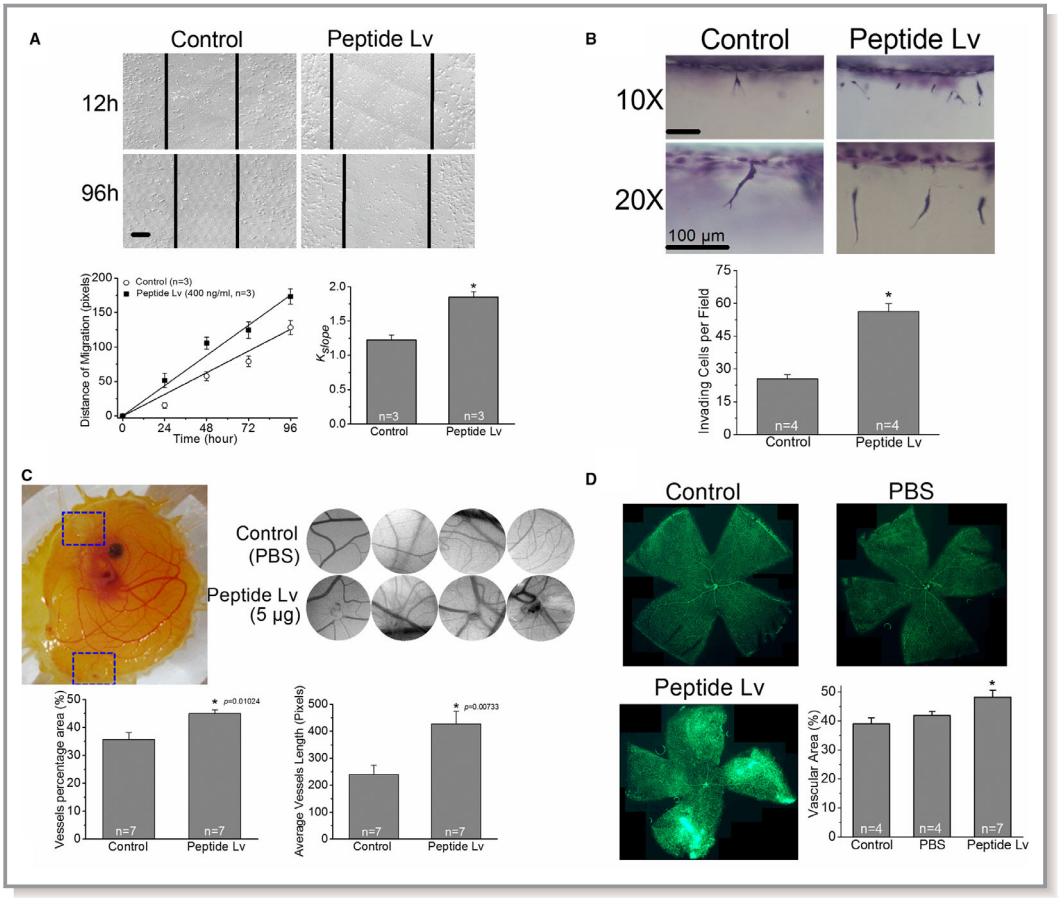

Figure 1. Peptide Lv promotes angiogenesis in vitro and in vivo. **A**, Peptide Lv promotes endothelial cell migration. The scratch-wound assays were carried out on cultured human RECs. Cells were treated with PBS (vehicle control) or peptide Lv (400 ng/mL) for 96 hours. The images were captured at 24 hour intervals with an inverted microscope (Olympus IX 71) at 10X (scale bar=200 μm). The migration distance (pixels) was plotted against time (hour) and fitted with linear regression. The cell migration is significantly enhanced by peptide Lv (*P=2.04×10^{-10} vs control; 2-way ANOVA with Fisher post hoc test; factor a: control vs peptide Lv; factor b: different time points; n=3 independent experiments; each experiment had triplicates). The higher K_{slope} reflects a faster migration rate. **B**, Peptide Lv enhances endothelial cell sprouting. The HUVECs were seeded onto collagen matrices containing 1 μmol/L sphingosine 1-phosphate with or without 400 ng/mL peptide Lv for the 3-dimensional sprouting/invasion assays. Cultures were fixed in 3% glutaraldehyde in PBS after 24 hours of invasion and stained with toluidine blue. Invasion density was quantified, and gels were photographed from the side. Photographs from one representative experiment showing invasion responses in collagen matrices taken at 10X and 20X were shown (scale bars=100 μm). Data represent the average number of invading cells per standardized field (0.25 mm^2). The cell sprouting is significantly increased by peptide Lv (*P=0.00453 vs control; Student t test; n=4 independent wells). **C**, Peptide Lv increases vascular growth in the chicken chorioallantoic membrane (CAM). The CAM angiogenesis assays were used to determine the effect of exogenous peptide Lv on angiogenesis during development. The shell-less cultures of chicken embryos started from embryonic day 2 to 3 (E2-3). At E11-12, the images of CAM areas treated with either synthetic peptide Lv (500 μg/mL, 10 μL) or PBS (vehicle control) were taken for further analyses. The dotted squares highlight the positions of coverslips where the covered areas were treated with peptide Lv or PBS in the shell-less culture. Representative images of vasculature under the whole coverslips from peptide Lv or PBS treated CAM areas are shown. The vascular area (vessels percentage area, %) and the average vessel length (pixels) are increased by peptide Lv (*P<0.05 vs Control; Student t test). **D**, Peptide Lv promotes the growth of retinal microvasculature in neonatal mice. A single intravitreal injection (2 μL) of peptide Lv (0.5 μg/μL) into one eye and PBS (vehicle control) into the contralateral eye was administered in neonatal mice at postnatal day 7 (P7). Four mouse eyes without any injections served as the negative control. At P12, the eyes were enucleated and fixed, and the whole mount retinas were stained with FITC-conjugated isolectin B4. The vascular areas were analyzed using the ImageJ software. Peptide Lv increases the growth of retinal microvessels in neonatal mice (*P=0.03016 vs control or PBS; 1-way ANOVA with Fisher post hoc test). FITC indicates fluorescein isothiocyanate; HUVECs, human umbilical vein endothelial cells; PBS, phosphate-buffered saline; REC, retinal endothelial cells.

served as the negative control. The proliferation of RECs was determined by the thiazolyl blue tetrazolium blue assay (Thermo Fisher Scientific). In brief, cells were incubated with the thiazolyl blue tetrazolium blue solution (1.2 mmol/L final concentration) for 4 hours at 37°C. Then 10% sodium dodecyl sulfate was added to break the plasma membrane, and the absorbance at 570 nm was measured with a spectrophotometer. Each experimental condition was repeated multiple trials (the "n"), and each trial was done in triplicate. The Chou-Talalay method[51] with their CompuSyn software[52] (www.combosyn.com) was used to analyze the synergism between VEGF and peptide Lv. According to Chou and Talalay,[51] "Fa" and "Fu" are the fractions of the system affected (Fa) and unaffected (Fu) by the drug combinations, where Fa+Fu equals 1, with Fa value between 0 and 1. A combination index (CI) value can quantitatively define combined effects between 2 or more drugs/treatments. A CI smaller than 1 in the Fa-CI plot represents a synergism in treatment combinations, a CI equal to 1 indicates an additive effect, while a CI larger than 1 signifies an antagonistic combination.

Quantitative Reverse Transcription Polymerase Chain Reaction

Total RNA from mouse retinas was isolated using a commercially available kit (Qiagen, Valencia, CA). One-step reverse transcription polymerase chain reaction amplification (Applied Biosystems/Life Technologies/Thermo Fisher Scientific) was used for the mRNA detection of peptide Lv precursor and β-actin as described previously.[32,33] The primers for peptide Lv: (sense) 5′-GAATTCATGCGGCTCCTAGCGCTGGCGGCGG-3′; (antisense) 5′-CTCGAGCTACAGCTGGTTCTCCTCGAAGAGGA-3′. The primers for mouse beta-actin: (sense) 5′-CAACGGCTCCGGCATGTGCAA-3′; (antisense) 5′-GTACATGGCTGGGGTGTTGAAGGTCTC-3′.

Western Blotting

The mouse spleens from the WT, $PLv^{+/-}$, and $PLv^{-/-}$ littermates were excised and homogenized in RIPA buffer supplemented with a mixture of protease inhibitors, 50 mmol/L NaF, and 1 mmol/L Na_3VO_4. The cell lysates were centrifuged, and the supernatants were denatured by 2X Laemmli sample buffer at 95°C for 10 minutes. Samples were separated on 10% sodium dodecyl sulfate–polyacrylamide gels by electrophoresis and transferred to nitrocellulose membranes. The primary antibodies used in this study were anti-Lv (rabbit polyclonal antibody, Biomatik, Ontario, Canada) and antipan actin (Cell Signaling Technology, Danvers, MA). Blots were visualized by using a goat-antirabbit secondary antibody conjugated to horseradish peroxidase (Cell Signaling Technology) and an enhanced chemiluminescence detection system (Thermo Fisher Scientific).

Laser-Induced CNV

Mice (C57BL/6J) were anesthetized with 100 mg/kg ketamine and 8 mg/kg xylazine intraperitoneally. Topical application of 0.5% tropicamide (Alcon, Fort Worth, TX) was applied to the eye for pupil dilation. Photocoagulation was performed as we previously described.[53] Briefly, each eye received 3 or 4 laser burns using a 532-nm wavelength laser (50 μm, 160 mW, 0.1 seconds) and a slit lamp (NIDEK, Fremont, CA). Animals were euthanized 3 weeks after laser photocoagulation. Immediately after laser photocoagulation, animals received an intravitreal injection of anti-Lv (2 μL, 1 μg/μL) in one eye and PBS (2 μL) in the contralateral eye as control. Spectral domain optical coherence tomography (SD-OCT) was performed using a Heidelberg Spectralis HRA+OCT (Heidelberg, Germany) as described previously.[53] For each CNV lesion, SD-OCT high-resolution horizontal and vertical scanning images were taken to calculate the volume of the CNV lesion.[54] The CNV volume was quantified using the Heidelberg Engineering software (Heidelberg Eye Explorer, Heidelberg, Germany) based on the ellipsoid volume formula.[54]

Fundus fluorescein angiography (FFA) was performed using the Heidelberg Spectralis HRA+OCT. Early- and late-phase FFA images were recorded at 1 to 5 and 15 to 25 minutes, after intraperitoneal injection of fluorescein sodium (10%, 0.15 mL; Alcon). Leakage was defined as the presence of an early hyperfluorescent spot that increased in size and/or intensity with time in the late-phase angiography.[55] The grade of leakage was assigned as described previously[53,56,57] from 0 (no leakage) to 3 (pathological significant leakage). Late-phase images were chosen for analysis of fluorescein leakage to correspond with the clearance time of fluorescein from the vasculature and to avoid interference with the observation of hyperfluorescence from CNV.[58]

For immunofluorescence and ex vivo CNV measurements, high-molecular-weight fluorescein isothiocyanate FITC-dextran (molecular weight 2×10^6 g/mol; Sigma-Aldrich) was administered through intracardiac injections (1 mL, 25 mg/mL) to mice under anesthesia. Animals were then euthanized, and eyes were enucleated and fixed in 4% formaldehyde for 30 minutes. The retina pigment epithelium-choroid-sclera complex was cut radially into 4 petals and then flat-mounted onto a slide and covered with a coverslip.[55] The flat-mount images were obtained with an Olympus microscope with epifluorescence (IX83; Olympus America, Waltham, MA). The CNV lesion area was analyzed with the cellSens image analysis software (Olympus). The CNV measurement data from the anti-Lv treatment were normalized to the average of the PBS group for comparison.

Ten mice (5 mice each group) were originally used in this study. Two eyes were later excluded from the data analysis due to vitreous hemorrhage, lack of hyperfluorescence in the

lesion sites, or merging of adjacent lesion sites, so each group had 9 eyes used for final data analyses.

Fundus Angiography

The fundus angiography on mice was performed as we previously described.[59] Mice were dark adapted for a minimum of 3 hours and anesthetized with Avertin solution (12.5 mg/mL) at a dosage of 500 μL per 25 g body weight. Pupils were dilated using a single drop of 1% tropicamide/2.5% phenylephrine mixture for 5 minutes. Mice were placed on a heating pad to maintain their body temperature at 37°C. A portable fundus scope (OcuScience, Henderson, NV) was used to record images of major blood vessels at the fundus. The vascular diameters were first measured at one optic disc diameter from the optic disc margin using the fundus images, and the artery/vein diameter ratios were compared.

Immunohistochemical Staining

The dog eye sections (diabetics and age-appropriate nondiabetics) were obtained from the archives of the Small Animal Hospital Pathology Laboratory in the College of Veterinary Medicine and Biomedical Sciences at Texas A&M University (College Station, TX). The human eye sections were obtained from Baylor Scott & White Hospital (Temple, TX) with institutional review board approval. The eyes from the high-fat-diet–induced diabetic mice and the control were excised and prepared as previously described.[60] After deparaffinization and antigen retrieval, sections were washed in PBS, locked with 10% goat serum for 2 hours at room temperature, and then incubated overnight with anti-Lv (1:1000 dilution) at 4°C. The next day, sections were washed with PBS several times and incubated with Alexa Fluor 488 goat antirabbit immunoglobulin G (IgG; 1:150 dilution; Thermo Fisher Scientific) for 2 hours at room temperature and mounted with ProLong Gold antifade reagent containing 4′,6-diamidino-2-phenylindole (Thermo Fisher Scientific). The epifluorescent images were captured on a Zeiss Stallion microscope (Carl Zeiss, AG). Each fluorescent image from each group was taken under identical settings, including the same exposure time and magnification.

Statistical Analysis

Data are reported as mean± SEM, and the n value represents the number of animals studied or in vitro experimental trials. The Student *t* test and 1- or 2-way ANOVA followed by Fisher post hoc test, or repeated measures 2-way ANOVA (for treatment and concentration factors) with Bonferroni multiple-range post hoc test (vasodilation experiments) were used to determine the significance of experimental interventions. The statistical software was Origin 9.0 (OriginLab, Northampton, MA) was used for most data analyses except the vasodilation and laser-induced CNV experiments, which were analyzed with Prism 8.0 (GraphPad Software, San Diego, CA). The specific statistical method used for each experiment is described in the figure legends. Throughout, $P<0.05$ was considered significant.

Results

Peptide Lv Promotes Endothelial Cell Migration and Sprouting In Vitro

Endothelial cell proliferation, migration, and sprouting are the 3 fundamental steps for angiogenesis.[61] As we previously showed that peptide Lv promotes endothelial cell proliferation,[33] here we tested whether peptide Lv was able to stimulate endothelial migration and sprouting using wound-healing assays[62] and 3-dimensional sprouting assays,[38] respectively. The migration rate was quantified by the slope after linear regression of the migration distance (pixels) of human RECs against time (hours; Figure 1A). Peptide Lv (400 ng/mL)-treated RECs had a significantly higher K_{slope} (1.85±0.08) compared with the vehicle control (PBS, vehicle; K_{slope}=1.22±0.08; Figure 1A) indicating that peptide Lv stimulated REC migration in vitro. Peptide Lv (400 ng/mL) also significantly promoted HUVEC sprouting and invasion in an assay using 3-dimensional collagen matrices (peptide Lv: 56±4 cells/field, control: 26±2 cells/field; Figure 1B). These results show that peptide Lv is able to promote angiogenesis in vitro.

Peptide Lv Promotes Developmental Angiogenesis in Chicken Embryos and Early Postnatal Mice

To examine the ability of peptide Lv to promote developmental angiogenesis in vivo, we first used the chorioallantoic membrane ex ovo assays and found that treatment with peptide Lv significantly increased the vascular area and average vessel length during embryonic development (Figure 1C). We then examined the effect of peptide Lv on retinal vascular development in early postnatal mice in vivo. The mouse retinal vasculature has a unique developmental pattern that makes it an excellent model to study factors affecting developmental and pathological angiogenesis.[37] At postnatal day 7 (P7), the capillaries from the superficial plexus initiate vertical sprouting into the deep retina layer; by P12, the deep capillary plexus is formed and extends to the peripheral retina; and around P21, the development of the retinal vasculature is

complete.[37] We injected one eye with peptide Lv (0.5 μg/μL, 2 μL), while the contralateral eye was injected with PBS (internal vehicle control) or without injection (control) at P7, harvested the retinas at P14, and analyzed the retinal vascular areas by staining whole mount retinas with FITC-conjugated isolectin-B4. Intravitreal injections with peptide Lv significantly increased the retinal vascular area (Peptide Lv: 48±2%) compared with the eyes without injections (control; 39±2%) or injected with PBS (vehicle; 42±1%; Figure 1D). This result implies that exogenous peptide Lv stimulates retinal vascular development in postnatal mice. Hence, peptide Lv promotes developmental angiogenesis in vivo.

Peptide Lv Dilates Coronary and Retinal Arterioles

In the early stage of angiogenesis, the dilation of existing vessels is an essential step to increase microvascular permeability and promote angiogenesis.[63,64] We previously showed that VEGF, via VEGFR2, is a potent endothelial NO-dependent vasodilator in coronary and retinal arterioles, because the NO synthase inhibitor L-NAME abolishes VEGF-elicited vasodilation.[35] Since peptide Lv was able to promote angiogenesis, we tested whether peptide Lv can elicit vasodilation. Peptide Lv elicited concentration-dependent vasodilations of isolated coronary (Figure 2A) and retinal arterioles (Figure 2B). However, in contrast to VEGF, peptide Lv-elicited vasodilations were only partially inhibited by L-NAME, suggesting an NO-independent component of vasodilation to peptide Lv. Therefore, peptide Lv might have both VEGFR2-dependent and -independent mechanisms in promoting angiogenesis, and the VEGFR2-independent target of peptide Lv remains unknown and requires future investigation.

The Angiogenic Action of Peptide Lv and VEGF Is Synergistic

If peptide Lv had VEGFR2-independent target(s), peptide Lv might function synergistically with VEGF in promoting angiogenic activities. Using the cell proliferation (thiazolyl blue tetrazolium blue colorimetric) assays with RECs, VEGF promoted REC proliferation in a concentration-dependent manner (Figure 2C), which was significantly enhanced in the presence of peptide Lv (100 ng/mL). We further used the Chou-Talalay method[51,52] with CompuSyn software to analyze the synergism between VEGF and peptide Lv. The combinations between peptide Lv (100 ng/mL) and VEGF (from 1 to 10 ng/mL) resulted in CI either being smaller than or close to 1 (Figure 2D), indicating that peptide Lv and VEGF are synergistic. Thus, it appears that peptide Lv is an angiogenic factor that functions similarly to VEGF in promoting angiogenesis in vitro and in vivo, as well as vasodilator action, in part, independent of VEGFR2.

Anti-Lv, an Antibody Specificically Against Peptide Lv Blocks Pathological Angiogenesis In Vivo

The upregulation of retinal VEGF and VEGFR2 in various ocular diseases especially DR, contributes to the neovascularization during disease progression.[20] We found that the expression of peptide Lv was also increased in the retinas of dogs with type 1 DR, human patients with early proliferated DR, and obesity-induced diabetic mice (Figure 3), indicating the possible involvement of peptide Lv in DR pathological angiogenesis. As such, an antibody against peptide Lv (anti-Lv) should diminish pathological angiogenesis, so we tested the effect of anti-Lv on VEGF-elicited endothelial proliferaion in vitro. Cultured HUVECs treated with VEGF (20 ng/mL) up to 96 hours had a signicantly higher proliferation compared with the vehicle control (Figure 4A). Treatment with anti-Lv at 50 or 100 μg/mL significantly decreased VEGF-elicited HUVEC proliferation (Figure 4A). Thus, anti-Lv has a potential to inhibit pathological angiogenesis in vivo. We next used OIR[37,44,65,66] and laser-induced CNV[67] mouse models to test whether intraocular injections of anti-Lv could block pathological angiogenesis. These models are the most used in vivo models for pathological angiogenesis: OIR is used to evaluate mechanisms involved in vascular retraction and neovascularization in developmental and early postnatal animals, and laser-induced CNV to determine mechanisms involved in neovascularization in adult animals.[44,68,69]

Peptide Lv mRNA was significantly increased in the retinas from OIR mice at P17 (Figure 4B). Intraocular injections with anti-Lv significantly inhibited pathological angiogenesis, as the vascular obliteration (vaso-obliteration) was significantly higher in eyes injected with anti-Lv compared with eyes injected with PBS (vehicle control) or peptide Lv (Figure 4C). Injections with peptide Lv significantly increased the level of neovascularization compared with the eyes injected with PBS or anti-Lv (Figure 4D). These findings indicate that oxygen-induced ocular pathological angiogenesis in the early postnatal stage is sensitive to peptide Lv blockage, and peptide Lv further stimulated pathological neovascularization.

We further tested the effect of anti-Lv on CNV progression. Immediately after laser photocoagulation, all animals received an intravitreal injection of anti-Lv (2 μL, 1 μg/μL) in the right eye and PBS (2 μL) in the left eye as the vehicle control. After 3 weeks, CNV size was assessed with SD-OCT and RPE-choroid-sclera flat mounts. Fluorescein leakage from CNV was graded by FFA. Intraocular injections

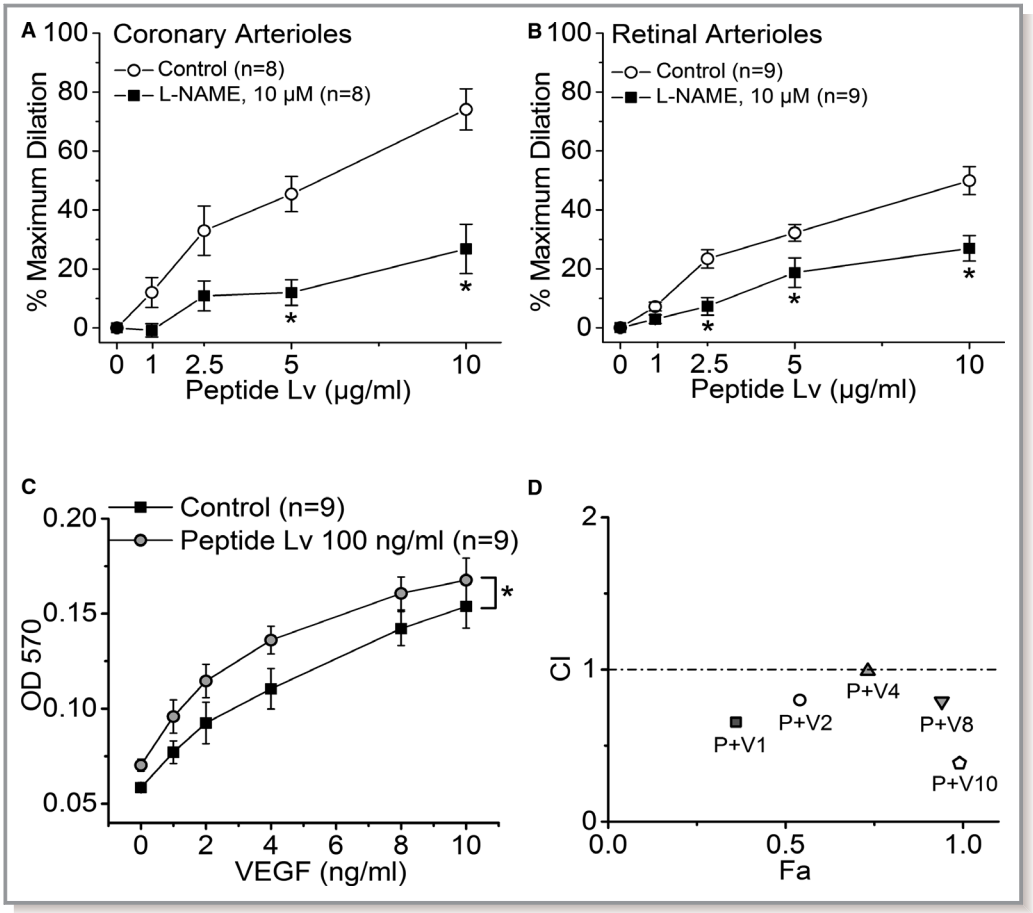

Figure 2. Peptide Lv elicits vasodilation and synergizes with VEGF. **A** and **B**, Peptide Lv stimulates dilation of coronary (**A**) and retinal (**B**) arterioles. Isolated coronary and retinal arterioles dilated in response to cumulative additions of peptide Lv (control). The concentration-dependent dilations of coronary and retinal arterioles to peptide Lv were only partially attenuated in the presence of L-NAME (*P<0.05 vs control. Repeated-measures 2-way ANOVA with Bonferroni multiple-range post hoc test was performed with factor a: control vs 10 μmol/L L-NAME, and factor b: varous concentrations of peptide Lv). **C**, Peptide Lv and VEGF are synergistic in promoting endothelial cell proliferation. Cultured human RECs were treated with VEGF at 1, 2, 4, 8, or 10 ng/mL without (control) or with 100 ng/mL peptide Lv (Peptide Lv) for 48 hours followed by the thiazolyl blue tetrazolium blue proliferation assays. There were 9 independent experimental trials (n=9) for each condition. Each experimental trial was done in triplicate. Two-way ANOVA with Fisher post hoc test was performed with factor a: control (VEGF only) vs peptide Lv 100 ng/mL, and factor b: various VEGF concentrations (overall *P=0.0003). **D**, The Chou-Talalay method with the CompuSyn software was used to analyze the synergism between VEGF and peptide Lv. V1, V2, V4, V8, and V10 represent treatments of VEGF at 1, 2, 4, 8, or 10 ng/mL, respectively, and P represents peptide Lv (100 ng/mL). The combination index (CI) and the fraction of the system affected (Fa) were plotted (0<Fa<1). The CI for various combinations of VEGF and peptide Lv in the Fa-CI plot is <1, representing the significance of synergism. (Fa, CI) data: P+V1: (0.36, 0.65); P+V2: (0.54, 0.80); P+V4: (0.73, 0.99); P+V8: (0.94, 0.79); P+V10: (0.99, 0.39). L-NAME indicates N(G)-nitro-L-arginine methyl ester; VEGF, vascular endothelial growth factor.

with anti-Lv significantly reduced the vascular fluorescein leakage in CNV lesions (Figure 5A) and the size of CNV by 50% with SD-OCT measurements (Figure 5B) and flat-mount analyses (Figure 5C; PBS vehicle: 36 965±7743 μm^2 versus anti-Lv: 15 738±2309 μm^2). These data demonstrate that anti-Lv is able to alleviate pathological angiogenesis in adult mice.

Genetic Deletion of Peptide Lv Affects the Microvasculature Only in Aging Animals and Worsens Pathological Neovascularization

Since anti-Lv dampened pathological angiogenesis in mice (Figures 4 and 5), we used genetic deletion of peptide Lv to investigate its role in developmental and pathological

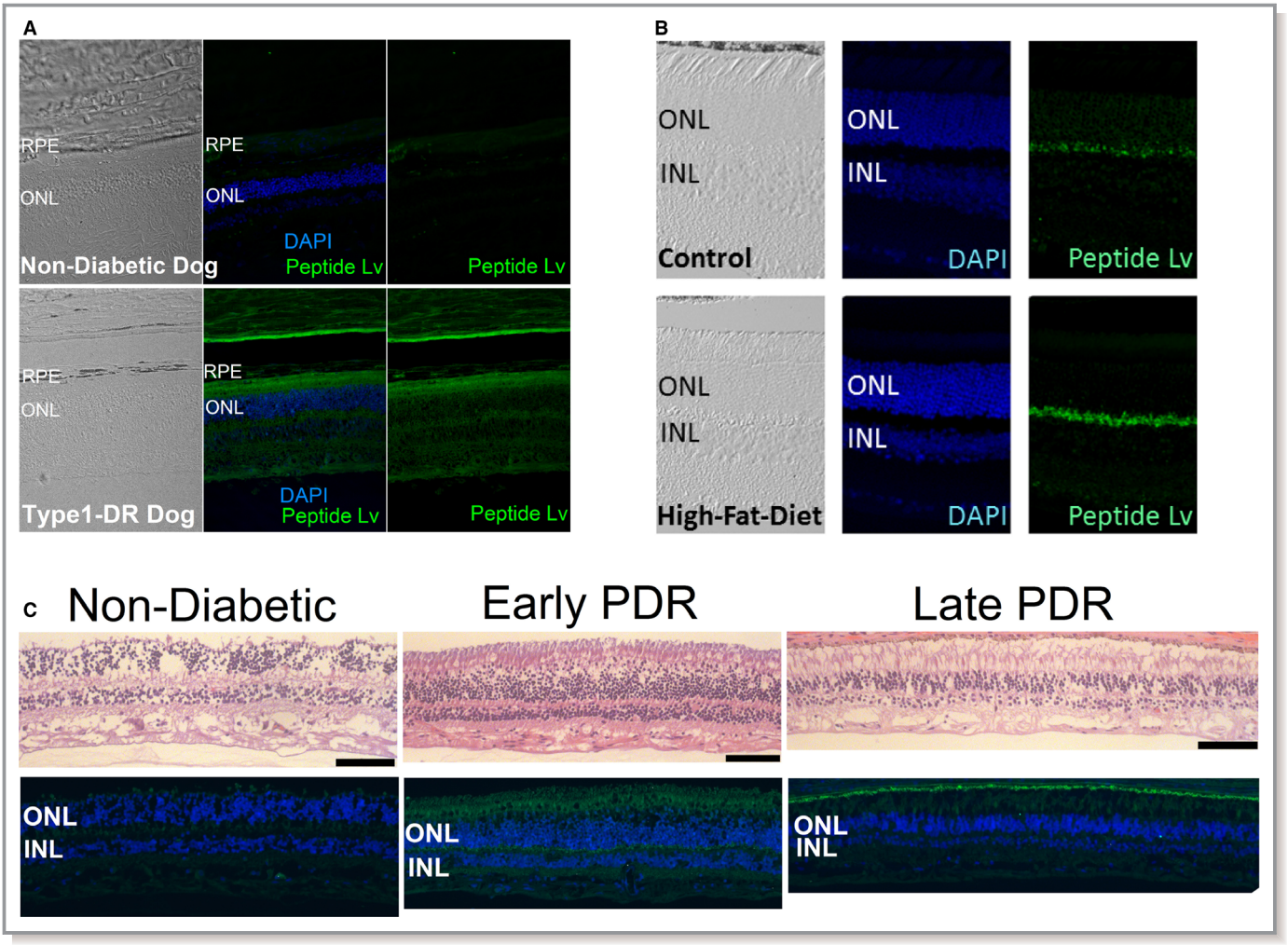

Figure 3. The expression of peptide Lv is increased in the DR retina. The eye sections were immuno-stained with a polyclonal antibody against peptide Lv (green fluorescence) and DAPI (blue, staining nuclei). **A**, The expression of peptide Lv was elevated in eye sections from dogs with type 1 diabetic retinopathy. **B**, Eye sections were from mice fed with normal chow (control) or a high-fat-diet (60% calories from fat) for 6 months as previously described.[60] Mice developed type 2 diabetes mellitus after 12 weeks of a high-fat diet, and the expression of peptide Lv in eye sections was upregulated. **C**, The human eye sections from patients with early proliferative diabetic retinopathy (PDR) or late PDR show the upregulation of peptide Lv (green fluorescence) compared with the age-appropriate nondiabetics (but with other abnormalities). Scale bar=100 μm. DAPI indicates 4′,6-diamidino-2-phenylindole; INL, inner nuclear layer; ONL, outer nuclear layer; RPE, retinal pigment epithelium.

angiogenesis. We generated peptide Lv null mice ($PLv^{-/-}$) using the CRISPR-cas9 technology to delete exon 2 of *Vstm4*, the gene encoding peptide Lv[32,33] (Figure 6A). Where VEGF and VEGFR2 null mice are embryonic lethal,[70,71] our $PLv^{-/-}$ mice lived to adulthood without any noticeable difference from their WT littermates in appearance. Analysis of fundus images showed that the artery/vein diameter ratios were not different among the WT, $PLv^{+/-}$, and $PLv^{-/-}$ mice at 4 to 6 months old (Figure 6B), indicating that there is no apparent retinal artery narrowing or vascular deficit in $PLv^{-/-}$ mice compared with their WT littermates. However, deletion of peptide Lv caused a significant decrease in the retinal vascular area compared with the WT littermates at 12 months but not 2 months old mice (Figure 6C). This suggests that peptide Lv might not be critical for developmental angiogenesis at young ages, but it is important in preventing vascular degeneration during aging. Furthermore, at P17, $PLv^{-/-}$ mice subjected to OIR had the highest vascular obliteration compared with the WT and $PLv^{+/-}$ littermates (Figure 7A). After analyzing the neovascular tufts. The $PLv^{+/-}$ and $PLv^{-/-}$ retinas had significantly lower neovascularization compared with the WT littermates (Figure 7B). These data indicate that deletion of peptide Lv significantly decreased neovascularization compared with the WT littermates. Thus, peptide Lv is important in maintaining vascular integrity in aged animals and is involved in pathological angiogenesis.

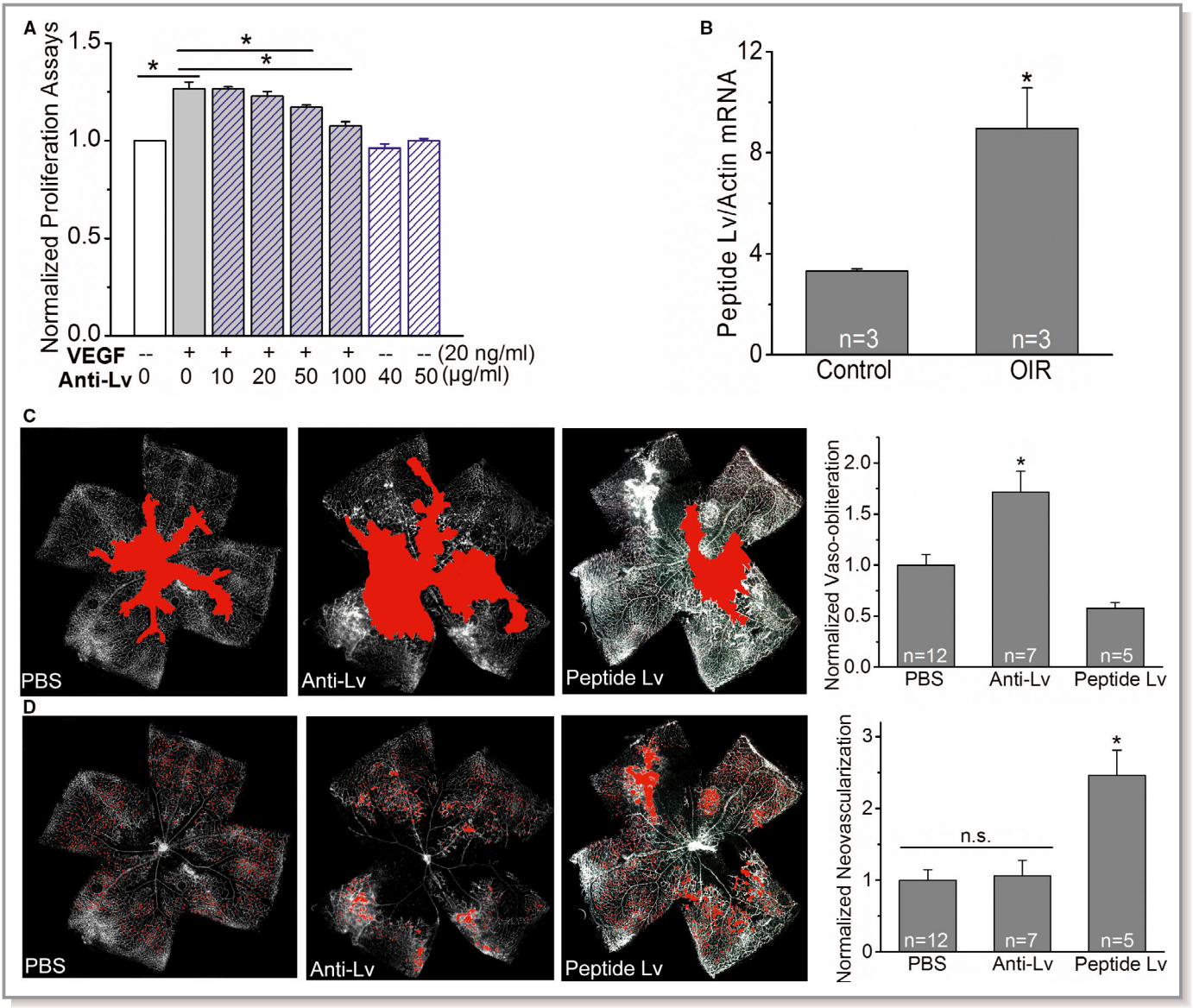

Figure 4. Anti-Lv dampens VEGF-elicited HUVEC proliferation in vitro and pathological angiogenesis in OIR in vivo. **A**, HUVECs were treated with VEGF (20 ng/mL) in the absence or presence of anti-Lv (10–100 μg/mL) for 96 hours. There were 3 independent experimental trials (n=3) for each condition. Each experimental trial was done in triplicate. VEGF significantly elicits HUVEC proliferation compared with the vehicle control (PBS treated). Treatment with anti-Lv at 50 or 100 μg/mL significantly dampens VEGF-elicited cell proliferation. Treatment with anti-Lv alone does not affect HUVEC proliferation. *A significant differences between VEGF vs control (without VEGF and anti-Lv), VEGF vs VEGF+anti-Lv (50 μg/mL), and VEGF vs VEGF+anti-Lv (100 μg/mL). *P<0.05; 1-way ANOVA with Fisher post hoc tests. **B** through **D**, Anti-Lv dampens but peptide Lv promotes pathological angiogenesis in the retinas with OIR. The neonatal mice from P7 to P12 were placed in a 75% oxygen chamber. At P12 upon returning to regular room air, a 2 μL of PBS (vehicle control), anti-Lv (2 μg), or peptide Lv (1 μg) was injected intraocularly. The retinas were excised at P17 for analyses. **B**, The retinas from the OIR mice (OIR) have a significant increase in the mRNA level of peptide Lv compared with the P17 mice without OIR (Control; *P=0.02479 vs control; Student t test). **C**, Intraocular injection with anti-Lv significantly increases vascular obliteration (vaso-obliteration) compared with the injection with PBS or peptide Lv (*P=0.00014 vs PBS and peptide Lv; 1-way ANOVA with Fisher's post hoc tests). **D**, The OIR eyes injected with peptide Lv have significantly higher tuft neovascularization (highlighted in red; *P=0.00062 vs PBS and anti-Lv; 1-way ANOVA with Fisher's post hoc tests). HUVECs indicates human umbilical vein endothelial cells; PBS, phosphate-buffered saline; OIR, oxygen-induced retinopathy; PBS, phosphate-buffered saline; VEGF, vascular endothelial growth factor.

Discussion

We previously showed that peptide Lv is able to bind to VEGFR2 and activate its downstream signaling.[33] It is not surprising that peptide Lv can mimic VEGF as a proangiogenic factor by stimulating endothelial cell proliferation,[33] migration, and sprouting in vitro as demonstrated in this report. We found that exogenous peptide Lv promoted angiogenesis in neonatal

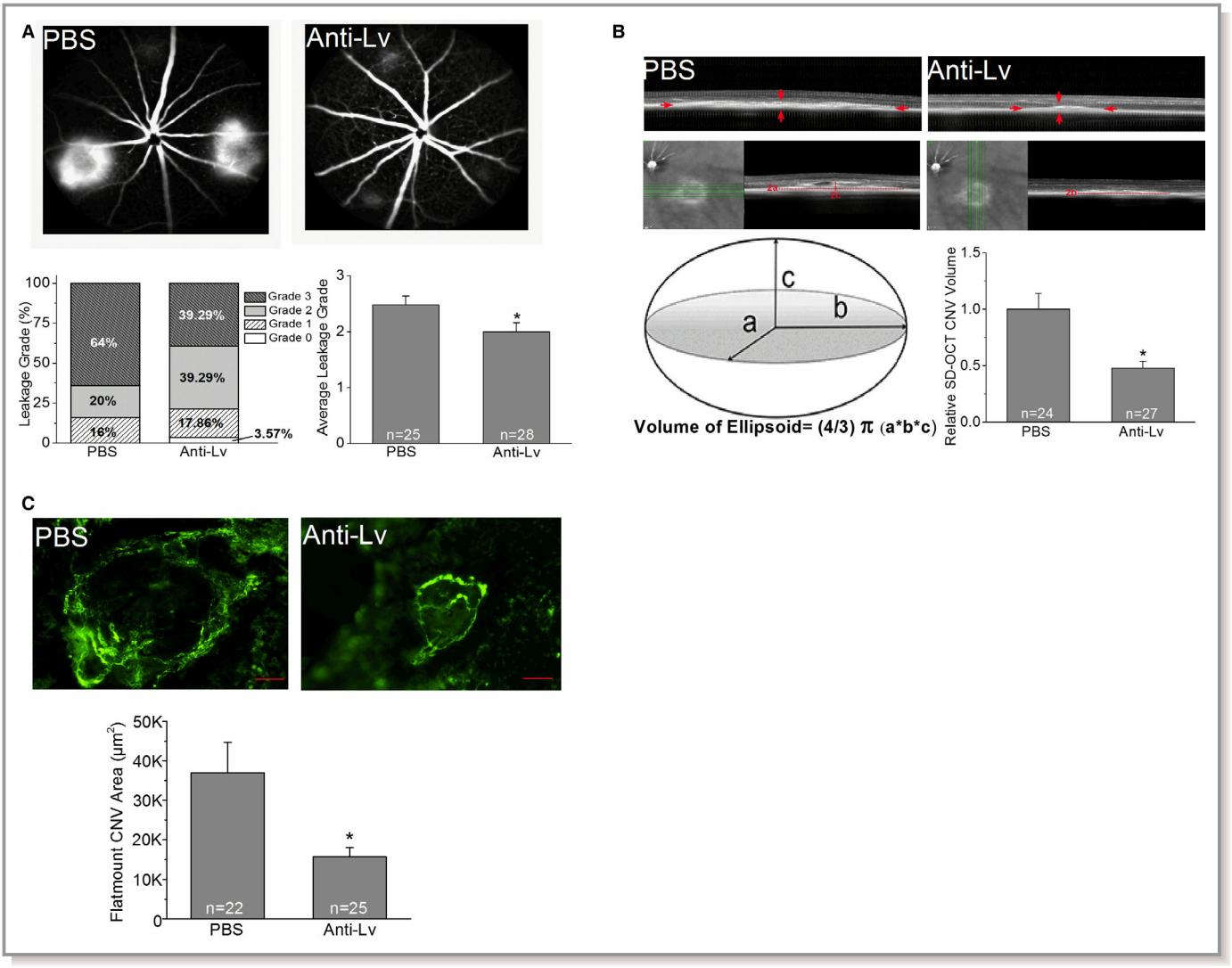

Figure 5. Anti-Lv decreases laser-induced CNV lesions. Ten eyes per group were originally used in this study. Each eye received 3 or 4 laser burns. Some eyes were excluded from the data analysis due to either vitreous hemorrhage, lack of hyperfluorescence in the lesion sites, or merging of adjacent lesion sites resulting in 9 eyes for each group used for final data analyses. The "n" represents the analyzed CNV lesion sites. **A**, The vascular leakage associated with laser-induced CNV lesions was assessed using FFA 3 weeks after laser photocoagulation. Representative FFA images of the control (laser-induced CNV+a single intravitreal injection with PBS) and the anti-Lv treated group (laser-induced CNV+a single intravitreal injection with anti-Lv) are shown. Treatment with anti-Lv significantly reduced the average leakage grade (2.0±0.16) compared with PBS (2.48±0.15; **P*=0.0366, Student *t* test). **B**, The volume of laser-induced CNV lesion sites were assessed with SD-OCT. The CNV lesions are spindle-shaped, hyper-reflective areas outlined by the *red arrows*. The width (2a), thickness (2c), and length (2b) of the CNV lesions were measured. The CNV volume was quantified based on the ellipsoid volume formula. The volume of the CNV lesions is significantly reduced in anti-Lv treated eyes (**P*=0.0009 vs PBS, Student *t* test). "n", number of lesion sites analyzed. **C**, Anti-Lv significantly decreases the areas of laser-induced CNV lesions in RPE-choroid-sclera flat mounts. Representative CNV lesions for the FITC-dextran-perfused RPE-choroid-sclera flat-mount of PBS or anti-Lv–treated eye are shown (scale bar=50 μm). Anti-Lv–treated eyes have significantly lower CNV-lesion areas compared with the PBS treated eyes (**P*=0.0081 vs PBS, Student *t* test). "n", the number of lesion sites analyzed. CNV indicates choroidal neovascularization; FFA, fundus fluorescein angiography; FITC, fluorescein isothiocyanate; PBS, phosphate-buffered saline; SD-OCT, spectral domain optical coherence tomography.

mice and chicken embryos in vivo. If the proangiogenic effect of peptide Lv were only through a VEGFR2-dependent manner, we would expect that peptide Lv would compete with VEGF in binding to VEGFR2 with a linear instead of bell-shaped Fa-CI plot, especially when VEGF was administered at higher concentrations (Figure 2D). Since peptide Lv and VEGF clearly showed synergistic effects at both high and low concentrations of VEGF, peptide Lv might have VEGFR2-independent targets to promote endothelial proliferation, and thus angiogenesis, when VEGFR2 is less available. In addition, VEGF through VEGFR2 elicits endothelial NO-dependent vasodilation.[35] But unlike VEGF, peptide Lv-elicited vasodilation was only partially

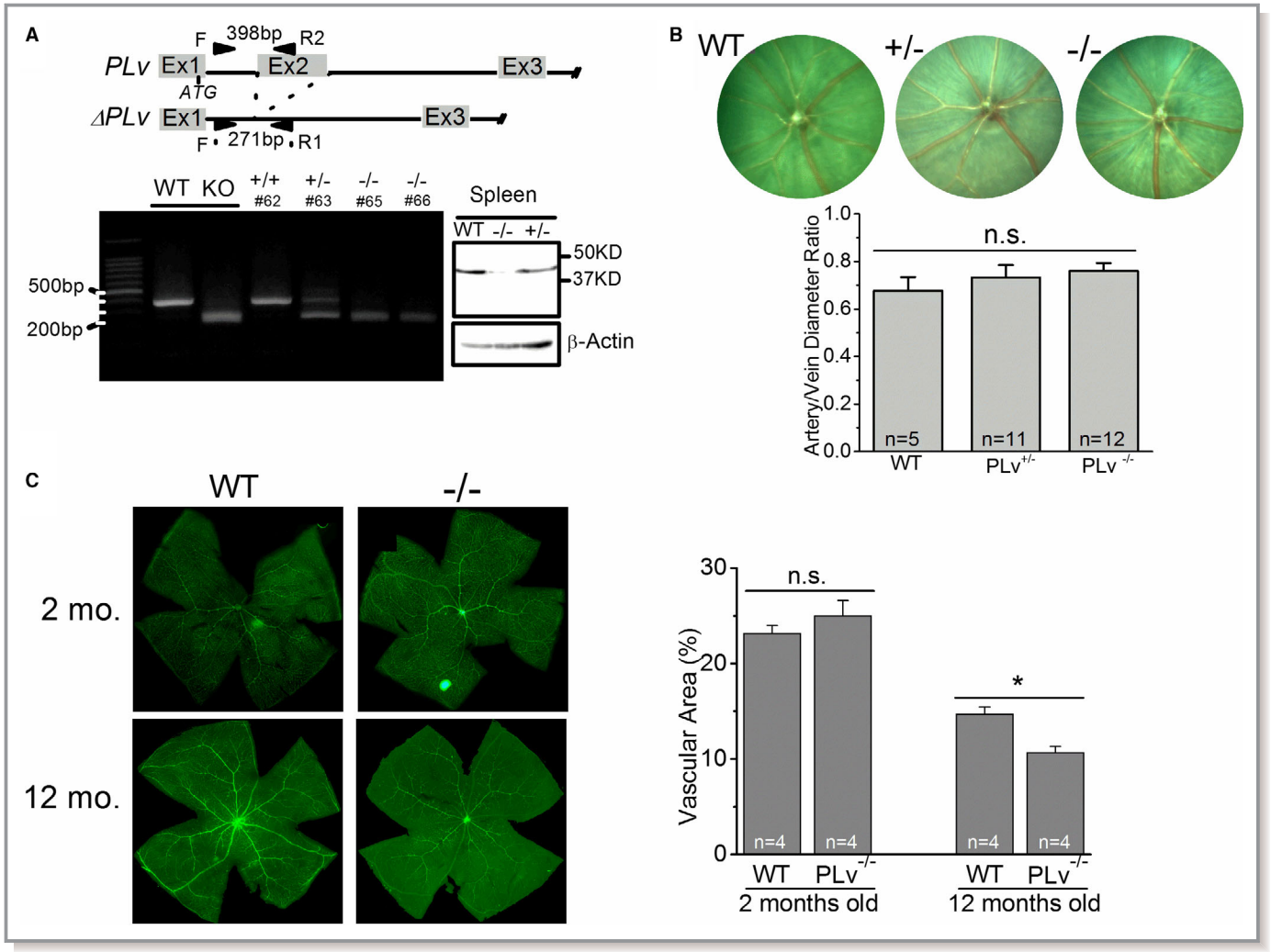

Figure 6. Genetic deletion of peptide Lv decreases retinal vasculature in aged mice. **A**, The CRISPR-Cas9 genetic editing method was used to genetically delete the peptide Lv precursor gene (*Vstm4*). The single-guide RNAs were designed to target the second exon (Ex2) of *Vstm4*. The polymerase chain reaction fragment was sequenced to confirm the successful deletion of exon 2. Western blotting was used to detect the expression of peptide Lv precursor in spleen samples from wild-type (WT), $PLv^{+/-}$ (heterozygeous; +/−), and $PLv^{-/-}$ (null; −/−) littermates. **B**, Peptide Lv null mice ($PLv^{-/-}$) do not have apparent vascular abnormalities under the fundus scope compared with their WT littermates at the same age (3–6 months old). The vascular diameters were measured at one optic disc diameter from the optic disc margin using the fundus images, and the artery/vein diameter ratios were compared. One-way ANOVA with Fisher post hoc test was used for statistical analysis. There is no significant difference (n.s.) in the artery/vein diameter ratio among the WT, $PLv^{+/-}$, and $PLv^{-/-}$ groups. **C**, Whole-mount retinas from 2 or 12 months old mice (WT and $PLv^{-/-}$) were stained with FITC-conjugated isolectin B4. The vascular areas were analyzed using the Angiotool software. The $PLv^{-/-}$ mice have significantly lower retinal vascular areas at 12 months old, but not 2 months old, compared with the WT littermates (*P<0.01 vs WT; Student t test). PBS indicates phosphate-buffered saline.

blocked by L-NAME, indicating that peptide Lv was able to elicit NO-dependent vasodilation maybe through VEGFR2, as well as NO-independent vasodilation via mechanisms yet to be discovered. These data suggest that peptide Lv may activate VEGFR2-independent vasodilation and angiogenesis, particularly on its role in the development of diseases associated with pathological angiogenesis, such as DR and age-related macular degeneration.

While we propose that peptide Lv might activate other signaling components in addition to VEGFR2, how peptide Lv cooperates with VEGF and activates VEGFR2 still remains unclear (Figure 8). Since there was a synergistic effect of peptide Lv and VEGF on endothelial cell proliferation, we postulated that peptide Lv could enhance VEGFR2 activities in endothelial cells through the following possibilities: (1) the interaction between peptide Lv and VEGFR2 might stabilize the cell membrane distribution of VEGFR2; (2) the interaction between peptide Lv and VEGFR2 might change the receptor conformation and further facilitate the binding of VEGF to VEGFR2 and accelerate VEGFR2 autophosphorylation; (3)

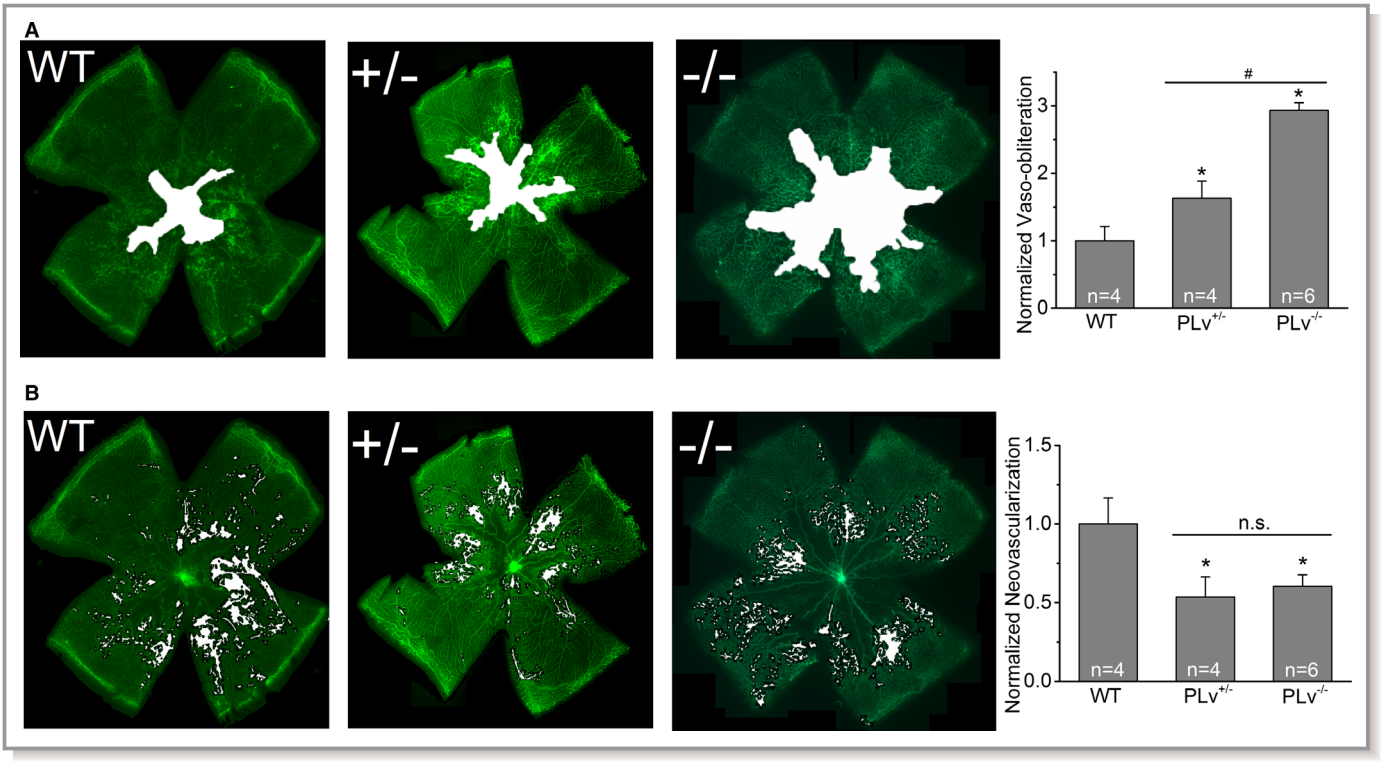

Figure 7. Deletion of peptide Lv exacerbates vascular loss in OIR eyes. The OIR mouse model was used to examine the role of endogenous peptide Lv in pathological angiogenesis. Mice (WT, $PLv^{+/-}$, and $PLv^{-/-}$) were placed in a 75% oxygen chamber from P7 to P12. At P17, the eyes were enucleated, and the whole mount retinas were stained with FITC conjugated isolectin B4. **A**, Both $PLv^{+/-}$ (+/−) and $PLv^{-/-}$ (−/−) groups have significantly higher vascular obliteration (vaso-obliteration; white area) compared with the WT littermates (*P<0.05; vs WT), and there is also a significant difference in vaso-obliteration between the $PLv^{+/-}$ and $PLv^{-/-}$ (#P<0.05). **B**, Both $PLv^{+/-}$ (+/−) and $PLv^{-/-}$ (−/−) mice have significantly lower tuft neovascularization (white area) compared with the WT littermates (*P<0.05), but there is no significant difference (n.s.) between the $PLv^{+/-}$ and $PLv^{-/-}$ mice on neovascularization. One-way ANOVA with Fisher post hoc test was used for statistical analysis (*P<0.05). OIR indicates oxygen-induced retinopathy; WT, wild-type.

peptide Lv might concurrently activate other VEGFR2-independent targets but eventually enhance the activation of the same downstream signaling; (4) peptide Lv might activate VEGFR2 through a noncanonical and VEGF-independent manner similar to other VEGFR2 activators such as galectin, gremlin, integrin β1, and CD63.[72–75] In addition to VEGF/VEGFR2, there are multiple pathways including fibroblast growth factor, matrix metalloproteinases, and Notch-signaling involved in the sprouting process of endothelial cells.[76–78] We cannot rule out the possibility that peptide Lv might activate one of these pathways to promote endothelial sprouting and angiogenesis. Hence, the ability of peptide Lv in promoting endothelial proliferation, migration, and sprouting renders the potential use of peptide Lv for therapeutic angiogenesis in wound healing, stroke, tissue ischemia, or cardiovascular diseases with the needs for revascularization. Future investigation in this area for clinical applications is needed.

We acknowledge that when comparing groups, statistical significance might be over stated due to correlation between samples from the same mouse, such as injecting one eye with PBS and the other eye with peptide Lv or anti-Lv. Nontheless, our results revealed that peptide Lv might play a significant role in pathological angiogenesis. The retinas from OIR mice had increased expression of peptide Lv mRNA, and the retinas from dogs and human patients with DR and from diabetic mice also had elevated peptide Lv, indicating that peptide Lv is upregulated under pathological conditions. In addition, anti-Lv dampened the neovascularization in OIR mice and decreased pathological angiogenesis and vascular leakage in mice with laser-induced CNV. Thus, the role of peptide Lv in pathological angiogenesis is similar to that of VEGF. However, unlike VEGF or VEGFR2 null mice that are embryonically lethal,[70,71] $PLv^{-/-}$ mice survived to adulthood and had normal retinal vasculature in young adults. But by 12 months old, these $PLv^{-/-}$ mice had significantly less retinal vasculature compared with their WT littermates. This implies that peptide Lv might be important for maintaining vascular integrity or preventing the loss of the retinal vasculature in mid-aged animals. Deletion of peptide Lv significantly exacerbated OIR-induced vascular obliteration and dampened OIR-induced neovascularization, which further supports our notion that peptide Lv plays a role in pathological angiogenesis.

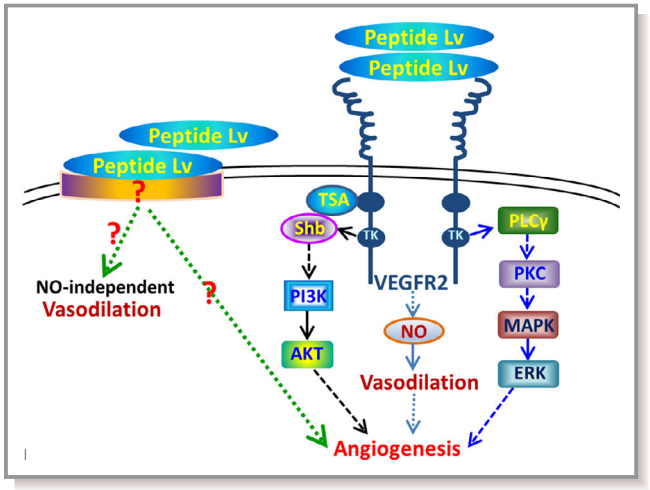

Figure 8. An illustration of peptide Lv and its downstream signaling. We previously showed that peptide Lv binds to and activates VEGFR2 and its downstream signaling. As VEGF via VEGFR2 elicits NO-dependent vasodilation, peptide Lv elicits NO-dependent and independent vasodilation. Other possible targets of peptide Lv require future investigations. AKT indicates protein kinase B; ERK, extracellular signal-regulated kinase; MAPK, mitogen-activated protein kinase; NO, nitric oxide; PI3K, phosphatidylinositol 3 kinase; PKC, protein kinase C; PLC, phospholipase C; Shb, the adaptor protein of VEGFR2; TK, tyrosine kinase; TSA, T-cell-specific adapter; VEGF, vascular endothelial growth factor; VEGFR2, vascular endothelial growth factor receptor 2.

Since upregulated VEGF and VEGFR2 are major contributors to diseases with pathological angiogenesis, especially in ocular neovascular diseases such as retinopathy of prematurity, age-related macular degeneration, and DR,[16] the anti-VEGF treatments are the most widely used therapy for treating these diseases.[79] Due to the resistance to anti-VEGFs as well as unwanted side effects in these therapies, more research has focused on discovering and managing novel proangiogenic factors for alternative therapeutics. As we unveiled peptide Lv and its function in angiogenesis and the effect of anti-Lv in mitigating pathological angiogenesis, there is a great therapeutic potential of developing anti-Lv against pathological neovascularization in the future.

Acknowledgments

We thank Dr. Brent Rocke at Baylor Scott and White Health for lending the laser machine to us for the CNV studies. We thank Drs. Andreas Stahl at Universitätsmedizin Greifswald and Lois Smith at Harvard Medical School for providing the SWIFT_NV macros. We thank Dr. Cathy C. Huang, Andy Kim, Wenjuan Xu and Xin Xu for technical support.

Sources of Funding

This study was supported by Texas A&M President's Excellence Fund-Triads for Transformation Seed Grant and Departmental Bridge Fund from Texas A&M University to Ko, Retinal Research Foundation and Kruse Family Endowed Chair Fund (Baylor Scott & White Health) to Kuo, and National Institutes of Health/National Eye Institute R01EY023335 and R01EY024624 to Hein.

Disclosures

None.

References

1. Campochiaro PA. Retinal and choroidal neovascularization. *J Cell Physiol*. 2000;184:301–310.
2. Okonkwo UA, DiPietro LA. Diabetes and wound angiogenesis. *Int J Mol Sci*. 2017;18:E1419.
3. Gurtner GC, Werner S, Barrandon Y, Longaker MT. Wound repair and regeneration. *Nature*. 2008;453:314–321.
4. Yehya AHS, Asif M, Petersen SH, Subramaniam AV, Kono K, Majid A, Oon CE. Angiogenesis: managing the culprits behind tumorigenesis and metastasis. *Medicina (Kaunas)*. 2018;54:8.
5. Sedding DG, Boyle EC, Demandt JAF, Sluimer JC, Dutzmann J, Haverich A, Bauersachs J. Vasa vasorum angiogenesis: key player in the initiation and progression of atherosclerosis and potential target for the treatment of cardiovascular disease. *Front Immunol*. 2018;9:706.
6. Oka T, Akazawa H, Naito AT, Komuro I. Angiogenesis and cardiac hypertrophy: maintenance of cardiac function and causative roles in heart failure. *Circ Res*. 2014;114:565–571.
7. Kobayashi K, Maeda K, Takefuji M, Kikuchi R, Morishita Y, Hirashima M, Murohara T. Dynamics of angiogenesis in ischemic areas of the infarcted heart. *Sci Rep*. 2017;7:7156.
8. Elshabrawy HA, Chen Z, Volin MV, Ravella S, Virupannavar S, Shahrara S. The pathogenic role of angiogenesis in rheumatoid arthritis. *Angiogenesis*. 2015;18:433–448.
9. Vouillarmet J, Bourron O, Gaudric J, Lermusiaux P, Millon A, Hartemann A. Lower-extremity arterial revascularization: is there any evidence for diabetic foot ulcer-healing? *Diabetes Metab*. 2016;42:4–15.
10. Nowak JZ. Age-related macular degeneration (AMD): pathogenesis and therapy. *Pharmacol Rep*. 2006;58:353–363.
11. Bressler NM, Bressler SB, Fine SL. Age-related macular degeneration. *Surv Ophthalmol*. 1988;32:375–413.
12. Nita M, Grzybowski A. The role of the reactive oxygen species and oxidative stress in the pathomechanism of the age-related ocular diseases and other pathologies of the anterior and posterior eye segments in adults. *Oxid Med Cell Longev*. 2016;2016:3164734.
13. Terry TL. Fibroblastic overgrowth of persistent tunica vasculosa lentis in infants born prematurely: II. Report of cases-clinical aspects. *Trans Am Ophthalmol Soc*. 1942;40:262–284.
14. Zhao M, Xie WK, Bai YJ, Huang LZ, Wang B, Liang JH, Yin H, Li XX, Shi X. Expression of total vascular endothelial growth factor and the anti-angiogenic VEGF b isoform in the vitreous of patients with retinopathy of prematurity. *Chin Med J*. 2015;128:2505–2509.
15. Cai X, McGinnis JF. Diabetic retinopathy: animal models, therapies, and perspectives. *J Diabetes Res*. 2016;2016:3789217.
16. Penn JS, Madan A, Caldwell RB, Bartoli M, Caldwell RW, Hartnett ME. Vascular endothelial growth factor in eye disease. *Prog Retin Eye Res*. 2008;27:331–371.
17. Bikfalvi A. Angiogenesis: health and disease. *Ann Oncol*. 2006;17(suppl 10):x65–x70.
18. Carmeliet P. Angiogenesis in health and disease. *Nat Med*. 2003;9:653–660.
19. Olsson AK, Dimberg A, Kreuger J, Claesson-Welsh L. VEGF receptor signalling—in control of vascular function. *Nat Rev Mol Cell Biol*. 2006;7:359–371.
20. Campochiaro PA. Ocular neovascularization. *J Mol Med (Berl)*. 2013;91:311–321.
21. Gallemore RP, Nguyen D. When anti-VEGF treatment fails. Review of Ophthalmology. Published by Jobson Medicail Information; March 20, 2008. Available at: http://www.reviewofophthalmology.com/content/d/retinal_insider/i/1230/c/23141/. Accessed April, 20, 2018.
22. Lux A, Llacer H, Heussen FM, Joussen AM. Non-responders to bevacizumab (Avastin) therapy of choroidal neovascular lesions. *Br J Ophthalmol*. 2007;91:1318–1322.

23. Palejwala NV, Lauer AK. Aflibercept: an update on recent milestones achieved. *Drugs Today (Barc)*. 2014;50:779–790.
24. Tranos P, Vacalis A, Asteriadis S, Koukoula S, Vachtsevanos A, Perganta G, Georgalas I. Resistance to antivascular endothelial growth factor treatment in age-related macular degeneration. *Drug Des Devel Ther*. 2013;7:485–490.
25. Seguin-Greenstein S, Lightman S, Tomkins-Netzer O. A meta-analysis of studies evaluating visual and anatomical outcomes in patients with treatment resistant neovascular age-related macular degeneration following switching to treatment with aflibercept. *J Ophthalmol*. 2016;2016:4095852.
26. Binder S. Loss of reactivity in intravitreal anti-VEGF therapy: tachyphylaxis or tolerance? *Br J Ophthalmol*. 2012;96:1–2.
27. Crawford Y, Kasman I, Yu L, Zhong C, Wu X, Modrusan Z, Kaminker J, Ferrara N. PDGF-C mediates the angiogenic and tumorigenic properties of fibroblasts associated with tumors refractory to anti-VEGF treatment. *Cancer Cell*. 2009;15:21–34.
28. Pili R, Chang J, Partis RA, Mueller RA, Chrest FJ, Passaniti A. The alpha-glucosidase I inhibitor castanospermine alters endothelial cell glycosylation, prevents angiogenesis, and inhibits tumor growth. *Cancer Res*. 1995;55:2920–2926.
29. Schnaper HW, Barnathan ES, Mazar A, Maheshwari S, Ellis S, Cortez SL, Baricos WH, Kleinman HK. Plasminogen activators augment endothelial cell organization in vitro by two distinct pathways. *J Cell Physiol*. 1995;165:107–118.
30. Stratmann A, Risau W, Plate KH. Cell type-specific expression of angiopoietin-1 and angiopoietin-2 suggests a role in glioblastoma angiogenesis. *Am J Pathol*. 1998;153:1459–1466.
31. Suri C, McClain J, Thurston G, McDonald DM, Zhou H, Oldmixon EH, Sato TN, Yancopoulos GD. Increased vascularization in mice overexpressing angiopoietin-1. *Science*. 1998;282:468–471.
32. Shi L, Ko ML, Abbott LC, Ko GY. Identification of peptide Lv, a novel putative neuropeptide that regulates the expression of L-type voltage-gated calcium channels in photoreceptors. *PLoS One*. 2012;7:e43091.
33. Shi L, Ko S, Ko ML, Kim AJ, Ko GY. Peptide Lv augments L-type voltage-gated calcium channels through vascular endothelial growth factor receptor 2 (VEGF2) signaling. *Biochim Biophys Acta*. 2015;1853:1154–1164.
34. Distler JH, Hirth A, Kurowska-Stolarska M, Gay RE, Gay S, Distler O. Angiogenic and angiostatic factors in the molecular control of angiogenesis. *Q J Nucl Med*. 2003;47:149–161.
35. Hein TW, Rosa RH Jr, Ren Y, Xu W, Kuo L. VEGF receptor-2-linked PI3K/Calpain/SIRT1 activation mediates retinal arteriolar dilations to VEGF and shear stress. *Invest Ophthalmol Vis Sci*. 2015;56:5381–5389.
36. Lokman NA, Elder AS, Ricciardelli C, Oehler MK. Chick chorioallantoic membrane (CAM) assay as an in vivo model to study the effect of newly identified molecules on ovarian cancer invasion and metastasis. *Int J Mol Sci*. 2012;13:9959–9970.
37. Stahl A, Connor KM, Sapieha P, Chen J, Dennison RJ, Krah NM, Seaward MR, Willett KL, Aderman CM, Guerin KI, Hua J, Lofqvist C, Hellstrom A, Smith LE. The mouse retina as an angiogenesis model. *Invest Ophthalmol Vis Sci*. 2010;51:2813–2826.
38. Bayless KJ, Kwak HI, Su SC. Investigating endothelial invasion and sprouting behavior in three-dimensional collagen matrices. *Nat Protoc*. 2009;4:1888–1898.
39. Cameron JS, Lhuillier L, Subramony P, Dryer SE. Developmental regulation of neuronal K^+ channels by target-derived TGF beta in vivo and in vitro. *Neuron*. 1998;21:1045–1053.
40. Cameron JS, Dryer L, Dryer SE. Regulation of neuronal K^+ currents by target-derived factors: opposing actions of two different isoforms of TGFbeta. *Development*. 1999;126:4157–4164.
41. Dunn BE, Fitzharris TP, Barnett BD. Effects of varying chamber construction and embryo pre-incubation age on survival and growth of chick embryos in shell-less culture. *Anat Rec*. 1981;199:33–43.
42. Finn TP, Kim S, Nishi R. Overexpression of ciliary neurotrophic factor in vivo rescues chick ciliary ganglion neurons from cell death. *J Neurobiol*. 1998;34:283–293.
43. West DC, Thompson WD, Sells PG, Burbridge MF. Angiogenesis assays using chick chorioallantoic membrane. *Methods Mol Med*. 2001;46:107–129.
44. Smith LE, Wesolowski E, McLellan A, Kostyk SK, D'Amato R, Sullivan R, D'Amore PA. Oxygen-induced retinopathy in the mouse. *Invest Ophthalmol Vis Sci*. 1994;35:101–111.
45. Stahl A, Connor KM, Sapieha P, Willett KL, Krah NM, Dennison RJ, Chen J, Guerin KI, Smith LE. Computer-aided quantification of retinal neovascularization. *Angiogenesis*. 2009;12:297–301.
46. Kuo L, Davis MJ, Chilian WM. Endothelium-dependent, flow-induced dilation of isolated coronary arterioles. *Am J Physiol*. 1990;259:H1063–H1070.
47. Hein TW, Yuan Z, Rosa RH Jr, Kuo L. Requisite roles of A_{2a} receptors, nitric oxide, and K_{ATP} channels in retinal arteriolar dilation in response to adenosine. *Invest Ophthalmol Vis Sci*. 2005;46:2113–2119.
48. Hein TW, Xu W, Kuo L. Dilation of retinal arterioles in response to lactate: role of nitric oxide, guanylyl cyclase, and ATP-sensitive potassium channels. *Invest Ophthalmol Vis Sci*. 2006;47:693–699.
49. Kuo L, Davis MJ, Chilian WM. Myogenic activity in isolated subepicardial and subendocardial coronary arterioles. *Am J Physiol*. 1988;255:H1558–H1562.
50. Hein TW, Qamirani E, Ren Y, Xu X, Thengchaisri N, Kuo L. Selective activation of lectin-like oxidized low-density lipoprotein receptor-1 mediates C-reactive protein-evoked endothelial vasodilator dysfunction in coronary arterioles. *Circ Res*. 2014;114:92–100.
51. Chou TC, Talalay P. Quantitative analysis of dose-effect relationships: the combined effects of multiple drugs or enzyme inhibitors. *Adv Enzyme Regul*. 1984;22:27–55.
52. Chou TC. Drug combination studies and their synergy quantification using the Chou-Talalay method. *Cancer Res*. 2010;70:440–446.
53. Zhao M, Xie W, Tsai SH, Hein TW, Rocke BA, Kuo L, Rosa RH Jr. Intravitreal stanniocalcin-1 enhances new blood vessel growth in a rat model of laser-induced choroidal neovascularization. *Invest Ophthalmol Vis Sci*. 2018;59:1125–1133.
54. Sulaiman RS, Quigley J, Qi X, O'Hare MN, Grant MB, Boulton ME, Corson TW. A simple optical coherence tomography quantification method for choroidal neovascularization. *J Ocul Pharmacol Ther*. 2015;31:447–454.
55. Cui J, Liu Y, Zhang J, Yan H. An experimental study on choroidal neovascularization induced by krypton laser in rat model. *Photomed Laser Surg*. 2014;32:30–36.
56. Liu T, Hui L, Wang YS, Guo JQ, Li R, Su JB, Chen JK, Xin XM, Li WH. In-vivo investigation of laser-induced choroidal neovascularization in rat using spectral-domain optical coherence tomography (SD-OCT). *Graefes Arch Clin Exp Ophthalmol*. 2013;251:1293–1301.
57. Ozone D, Mizutani T, Nozaki M, Ohbayashi M, Hasegawa N, Kato A, Yasukawa T, Ogura Y. Tissue plasminogen activator as an antiangiogenic agent in experimental laser-induced choroidal neovascularization in mice. *Invest Ophthalmol Vis Sci*. 2016;57:5348–5354.
58. Guthrie MJ, Osswald CR, Valio NL, Mieler WF, Kang-Mieler JJ. Objective area measurement technique for choroidal neovascularization from fluorescein angiography. *Microvasc Res*. 2014;91:1–7.
59. Kim AJ, Chang JY, Shi L, Chang RC, Ko ML, Ko GY. The effects of metformin on obesity-induced dysfunctional retinas. *Invest Ophthalmol Vis Sci*. 2017;58:106–118.
60. Chang RC, Shi L, Huang CC, Kim AJ, Ko ML, Zhou B, Ko GY. High-fat diet-induced retinal dysfunction. *Invest Ophthalmol Vis Sci*. 2015;56:2367–2380.
61. Risau W. Mechanisms of angiogenesis. *Nature*. 1997;386:671–674.
62. Rodriguez LG, Wu X, Guan JL. Wound-healing assay. *Methods Mol Biol*. 2005;294:23–29.
63. Conway EM, Collen D, Carmeliet P. Molecular mechanisms of blood vessel growth. *Cardiovasc Res*. 2001;49:507–521.
64. Hood JD, Meininger CJ, Ziche M, Granger HJ. VEGF upregulates ecNOS message, protein, and NO production in human endothelial cells. *Am J Physiol*. 1998;274:H1054–H1058.
65. Shih SC, Ju M, Liu N, Smith LE. Selective stimulation of VEGFR-1 prevents oxygen-induced retinal vascular degeneration in retinopathy of prematurity. *J Clin Invest*. 2003;112:50–57.
66. Wesolowski E, Smith LE. Effect of light on oxygen-induced retinopathy in the mouse. *Invest Ophthalmol Vis Sci*. 1994;35:112–119.
67. Lambert V, Lecomte J, Hansen S, Blacher S, Gonzalez ML, Struman I, Sounni NE, Rozet E, de Tullio P, Foidart JM, Rakic JM, Noel A. Laser-induced choroidal neovascularization model to study age-related macular degeneration in mice. *Nat Protoc*. 2013;8:2197–2211.
68. Smith LE. Pathogenesis of retinopathy of prematurity. *Acta Paediatr Suppl*. 2002;91:26–28.
69. Nowak-Sliwinska P, Alitalo K, Allen E, Anisimov A, Aplin AC, Auerbach R, Augustin HG, Bates DO, van Beijnum JR, Bender RHF, Bergers G, Bikfalvi A, Bischoff J, Bock BC, Brooks PC, Bussolino F, Cakir B, Carmeliet P, Castranova D, Cimpean AM, Cleaver O, Coukos G, Davis GE, De Palma M, Dimberg A, Dings RPM, Djonov V, Dudley AC, Dufton NP, Fendt SM, Ferrara N, Fruttiger M, Fukumura D, Ghesquiere B, Gong Y, Griffin RJ, Harris AL, Hughes CCW, Hultgren NW, Iruela-Arispe ML, Irving M, Jain RK, Kalluri R, Kalucka J, Kerbel RS, Kitajewski J, Klaassen I, Kleinmann HK, Koolwijk P, Kuczynski E, Kwak BR, Marien K, Melero-Martin JM, Munn LL, Nicosia RF, Noel A, Nurro J, Olsson AK, Petrova TV, Pietras K, Pili R, Pollard JW, Post MJ, Quax PHA, Rabinovich GA, Raica M, Randi AM, Ribatti D, Ruegg C, Schlingemann RO, Schulte-Merker S, Smith LEH, Song JW, Stacker SA, Stalin J, Stratman AN, Van de Velde M, van Hinsbergh VWM, Vermeulen PB,

Waltenberger J, Weinstein BM, Xin H, Yetkin-Arik B, Yla-Herttuala S, Yoder MC, Griffioen AW. Consensus guidelines for the use and interpretation of angiogenesis assays. *Angiogenesis*. 2018;21:425–532.

70. Carmeliet P, Ferreira V, Breier G, Pollefeyt S, Kieckens L, Gertsenstein M, Fahrig M, Vandenhoeck A, Harpal K, Eberhardt C, Declercq C, Pawling J, Moons L, Collen D, Risau W, Nagy A. Abnormal blood vessel development and lethality in embryos lacking a single VEGF allele. *Nature*. 1996;380:435–439.
71. Ferrara N, Carver-Moore K, Chen H, Dowd M, Lu L, O'Shea KS, Powell-Braxton L, Hillan KJ, Moore MW. Heterozygous embryonic lethality induced by targeted inactivation of the VEGF gene. *Nature*. 1996;380:439–442.
72. Markowska AI, Jefferies KC, Panjwani N. Galectin-3 protein modulates cell surface expression and activation of vascular endothelial growth factor receptor 2 in human endothelial cells. *J Biol Chem*. 2011;286:29913–29921.
73. Mitola S, Ravelli C, Moroni E, Salvi V, Leali D, Ballmer-Hofer K, Zammataro L, Presta M. Gremlin is a novel agonist of the major proangiogenic receptor VEGFR2. *Blood*. 2010;116:3677–3680.
74. Tugues S, Honjo S, Konig C, Padhan N, Kroon J, Gualandi L, Li X, Barkefors I, Thijssen VL, Griffioen AW, Claesson-Welsh L. Tetraspanin CD63 promotes vascular endothelial growth factor receptor 2-beta1 integrin complex formation, thereby regulating activation and downstream signaling in endothelial cells in vitro and in vivo. *J Biol Chem*. 2013;288:19060–19071.
75. Domigan CK, Ziyad S, Iruela-Arispe ML. Canonical and noncanonical vascular endothelial growth factor pathways: new developments in biology and signal transduction. *Arterioscler Thromb Vasc Biol*. 2015;35:30–39.
76. Park C, Kim TM, Malik AB. Transcriptional regulation of endothelial cell and vascular development. *Circ Res*. 2013;112:1380–1400.
77. Herbert SP, Stainier DY. Molecular control of endothelial cell behaviour during blood vessel morphogenesis. *Nat Rev Mol Cell Biol*. 2011;12:551–564.
78. Hellstrom M, Phng LK, Hofmann JJ, Wallgard E, Coultas L, Lindblom P, Alva J, Nilsson AK, Karlsson L, Gaiano N, Yoon K, Rossant J, Iruela-Arispe ML, Kalen M, Gerhardt H, Betsholtz C. Dll4 signalling through Notch1 regulates formation of tip cells during angiogenesis. *Nature*. 2007;445:776–780.
79. Rosenfeld PJ, Brown DM, Heier JS, Boyer DS, Kaiser PK, Chung CY, Kim RY; Group MS. Ranibizumab for neovascular age-related macular degeneration. *N Engl J Med*. 2006;355:1419–1431.